Journal of *Marine Science and Engineering*

MDPI

Article

Multi-Objective Optimization of Ship Design for the Effect of Wind Propulsion †

Timoleon Plessas * and Apostolos Papanikolaou

Ship Design Laboratory, National Technical University of Athens,15772 Athens, Greece; papa@deslab.ntua.gr

* Correspondence: timplessas@naval.ntua.gr

† This paper is an extended version of our paper published in Plessas, T.; Papanikolaou, A. Optimization of Ship Design for the Effect of Wind Propulsion. In Proceedings of the 15th International Marine Design Conference (IMDC-2024), Amsterdam, The Netherlands, 2–6 June 2024.

Abstract: International regulations and market demand for zero-emission transportation are accelerating the adoption of sustainable solutions in the shipping industry. Wind-Assisted Propulsion Systems (WAPSs) present a promising alternative, as elaborated on in the EU-funded Orcelle Wind project. This paper deals with the integration of wing sails into the conceptual design of a Very Large Crude Carrier (VLCC) using a parametric, multi-objective optimization framework. The results reveal that optimized VLCC designs with WAPSs can achieve over 20% reductions in fuel consumption and greenhouse gas emissions compared to conventional designs. Additionally, the obtained optimized designs exhibit notable differences in the main design characteristics and hull form compared to conventional designs, highlighting the importance of multi-objective optimization in the early design stage to tap the potential of WAPS technologies and wind propulsion.

Keywords: ship design; parametric optimization; wind propulsion; wing sails; WAPS; case study

Academic Editor: Decheng Wan

Received: 25 December 2024
Revised: 13 January 2025
Accepted: 16 January 2025
Published: 18 January 2025

Citation: Plessas, T.; Papanikolaou, A. Multi-Objective Optimization of Ship Design for the Effect of Wind Propulsion. *J. Mar. Sci. Eng.* **2025**, *13*, 167. https://doi.org/10.3390/jmse13010167

1. Introduction

The International Windship Association (IWSA) has declared 2021–2030 as the 'Decade of Wind Propulsion', and the European Maritime Safety Agency (EMSA) recently released a report [1] concluding that "wind-assisted propulsion is considered to have potential for the shipping industry". This suggests a resurgence of interest in wind propulsion, as the maritime sector explores Wind-Assisted Propulsion Systems (WAPSs) to significantly reduce its carbon footprint. With numerous regulatory requirements concerning greenhouse gas (GHG) emissions [2–4], along with rising costs and logistical challenges related to green fuels, wind propulsion emerges as a promising alternative. It not only offers a pathway to meet environmental goals and comply with regulations but also helps lower operational costs. Wind is a freely available, future-proof energy source, unaffected by the price fluctuations of conventional or alternative fuels. Furthermore, it is a reliable energy source with zero emissions, requiring no new shore-based infrastructure or logistics systems, and stands as one of the few technologies capable of providing significant fuel and emission savings.

Thus, WAPSs are emerging as a key solution for reducing emissions in the maritime industry. These systems, which harness wind energy to assist or replace conventional propulsion, are classified into several categories including rotors, rigid sails, suction wings, soft sails, and kites. Each technology varies in design, cost, and effectiveness, with rotor sails and rigid wings being the most widely implemented.

Despite the relatively early stage of adoption, more vessels are integrating WAPSs since they provide significant fuel savings and reduce emissions, though they are typically used in hybrid configurations rather than as primary propulsion. According to IWSA [5], the number of commercial vessels equipped with wind propulsion technology continues to rise. As of August 2023, a total of 30 large ships across various sectors, including VLCCs/VLOCs, other tankers and bulk carriers, ro-ro vessels, ferries, and general cargo ships, were outfitted with wind propulsion systems. Additionally, eight ships were designated as 'wind-ready'. These vessels collectively featured 63 wind propulsion rigs and represented over 1.8 million tonnes of shipping capacity (measured in terms of DWT for cargo ships and gross tonnage (GT) for passenger and ro-ro vessels) at that time. Furthermore, another 445,000 DWT is 'wind-ready', with 16 additional ships (totaling 1.7 million DWT) being installed and delivered within 2024.

The potential for fully wind-powered large cargo vessels is still a future goal, requiring further innovation and integration with other measures like alternative fuels. However, WAPSs are a critical part of the broader effort to decarbonize shipping and meet international emission reduction targets.

Recent and older studies have extensively modeled and simulated Wind-Assisted Propulsion Systems [6–8], with potential fuel savings demonstrated through simulation methods of 3 Degrees Of Freedom (DOF) [9,10], which examines vessel motion in the surge, sway, and yaw directions, and 4-DOF [11], which examines vessel motions in surge, sway, yaw, and roll directions. While the focus has largely been on performance predictions for vessels equipped with WAPSs, the selection of the appropriate WAPSs for specific vessels and routes [12], and/or the optimization of the design characteristics of WAPSs [13], the impact of WAPSs on the early-stage ship design optimization has yet to be systematically studied. Recently, Hao et al. [14] demonstrated the optimization of local hull parameters for minimizing resistance and wake field using Computational Fluid Dynamics (CFD) of a VLCC fitted with a WAPS. In practice, so far, traditional ship designs have primarily been retrofitted with WAPSs, and their performance assessed or optimized, ignoring that there will be an effect of WAPSs on the main characteristics in the initial ship design.

This paper is a revised and expanded version of a previously released publication by the authors [15] and presents the development of a parametric multi-objective ship design optimization framework to identify potential variations in the main dimensions and characteristics of ships when incorporating WAPSs. The present study refers to the concept design of ships fitted with wing sails, but other WAPSs (Fletner rotors, etc.) can be readily considered by the developed software tool. It is important to note that up to now, WAPSs have been applied to ships mainly as retrofits to existing designs, even in the case of newly built ships. To address this, we have developed and implemented a new methodology in MATLAB (version 2024a) [16] that facilitates the rapid simulation of the impact of different WAPSs on the design of ships of various types and sizes. This method identifies trends in key ship design parameters (main dimensions, hull form, main engine, and propeller characteristics), while taking into account all relevant major design constraints (like stability, longitudinal strength, freeboard), using only a few input parameters. The methodology and software tool are applied here to the concept design of a VLCC tanker with a WAPS (specifically, equipped with generic wing sails) to demonstrate the applicability and limitations of the approach. The main advantages of the herein-developed method, and the associated software tool, compared to other studies are as follows:

- It allows the optimization of the design of vessels fitted with WAPSs from scratch at the concept design stage (not as a retrofit solution to an existing design).
- It is a flexible and modular MATLAB tool allowing the consideration of different ship types, sizes, and WAPSs.

- It is fully parametric, while beyond the eight selected variables that are presented in this paper, more optimization variables can be incorporated in the optimization study, such as propeller diameter, number of propeller blades, vessel speed (laden and ballast), WAPS alternative technologies, etc., which can be optimized for any given routes.
- It allows single- and multi-objective optimization.
- It allows optimization of the hull form, engine, propeller, and sail design characteristics in parallel, within the same optimization framework.

2. WAPS Simulation Tool

2.1. Wind-Powered Ship Propulsion Simulation Model

In this study, we focus on the concept design of ships equipped with WAPSs, using a simplified one-degree-of-freedom (1-DOF) hydrodynamic simulation model to assess the impact of WAPSs on ship design. The primary distinction between a 1-DOF model (which accounts for surge, or movement in the longitudinal direction) and a 4-DOF model (which includes surge, sway, yaw, and roll movements) lies in the inclusion of additional hydrodynamic forces. These additional forces arise from the rudder resistance required to maintain the desired course, as well as the drift resistance and induced yaw moment, which occur when the vessel sails at a drift angle, leading to non-symmetrical flow around the hull. To address the lack of roll motion in the 1-DOF model, we employ a simplified approach that calculates the induced heel angle hydrostatically, namely by estimating the static heel based on the generated sail side force. Additionally, the influence of the heel angle on the projected sail area and the height of the center of effort is considered. While this method provides a simplified solution, it omits dynamic phenomena associated with a full maneuvering model of the ship's hydrodynamics [17] and should be applied cautiously in situations where significant heel angles or the hydrodynamic effects of hull appendages (e.g., bilge keels, sideboards, or bottom daggerboards) are important. A case study by Tillig and Ringsberg [11], examining the use of WAPSs on a tanker operating between Gothenburg and St. Petersburg in the Baltic Sea, found that fuel consumption estimates for wind-assisted vessels using a 1-DOF model differed from those using a 4-DOF model by between merely 2% (for smaller sail areas, e.g., 300 m^2) to 7% (for larger sail areas, e.g., 900 m^2), with the 4-DOF model providing more conservative saving predictions.

Following this reasoning and for the purpose of optimizing the ship's concept design, a one-degree-of-freedom (1-DOF), quasi-steady model has been developed and coded for simulating and optimizing a ship operating in a predefined route with available weather data information. The developed model takes into account the interaction between the hull, propeller, engine, and sail, simulates and balances all forces in the surge direction, and estimates the power and fuel consumption needed to complete a scheduled voyage (Figure 1). In addition, the developed model allows communication (exchange of data) between MATLAB and the more advanced NAPA (version 2021.2-1) naval architectural software package [18]. This enables the conduct of a more detailed analysis for each generated design alternative, which includes lightship and loading condition determination, intact stability criteria assessment, environmental regulation assessment (e.g., oil outflow compliance for tankers), and overall performance analysis. The user can choose when NAPA should be utilized during the optimization. Alternatively, simplified calculations can be conducted within MATLAB without the need to use NAPA, which may provide fewer details but it significantly speeds up the optimization procedure. Indicatively, when using NAPA, a single simulation takes approximately 40 s, whereas computations using semi-empirical formulas within MATLAB take approximately 1 s on a conventional computer. The results presented in this study were conducted using only MATLAB internal routines.

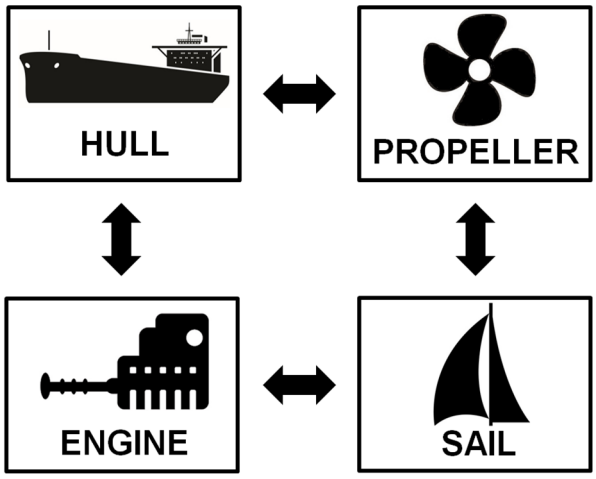

Figure 1. MATLAB code: interaction between vessel modules.

To optimize the ship's concept design, a one-degree-of-freedom (1-DOF), quasi-steady model has been developed and implemented for simulating and optimizing a ship operating on a predefined route using available weather data. The model accounts for the interactions between the hull, propeller, engine, and sail, balancing all forces in the surge direction to estimate the power and fuel consumption required to complete a scheduled voyage.

The developed simulation tool is composed of three core modules: "Input Creation", "Simulation", and "Output". The "Input Creation" module generates all the necessary inputs, such as power curves, engine performance curves, stability and weight relationships, and calculations, while considering the selected design variables (for more details, refer to the "Design Variables" subsection). Once the required input files are generated, the "Simulation" module computes the hydrodynamic and aerodynamic forces acting on the vessel and simulates its operation on the selected route, factoring in available weather data (wind and waves). Finally, the "Output" module handles the presentation of results, producing the relevant figures and tables.

In the case study under consideration, the voyage follows a typical tanker route from Corpus Christi (USA) to Rotterdam (the Netherlands) (Figure 2). The voyage is divided into 12 segments, assuming it is a round trip, with the vessel sailing loaded with cargo ("laden" condition) and returning with an empty load ("ballast" condition) along the same route, resulting in a total of 24 legs (12 for the laden condition and 12 for the ballast condition). For each leg, the relevant parameters are calculated twice: once factoring in the effect of the wing sails, and once assuming the wing sails are absent/folded, maintaining a fixed speed. This approach enables a direct comparison of the impact of the wing sails on the required thrust to propel the vessel, providing the basis for the optimization process in which the influence of the wing sails on ship design is analyzed.

The performance of WAPSs depends greatly on the wind characteristics of the route, particularly on the prevailing wind direction and strength, which vary by location, time, and season. As a result, the shortest route between the departure and arrival points is not always the most optimal, and traditional routing optimization tools must account for the best wind potential along the route. To address this, SSPA/RISE has developed an optimal routing methodology that allows for the assessment of operational energy savings across various global trading routes. This methodology takes into account the vessel's need to integrate into a logistics system, considering factors such as arrival time and lateness, and incorporates weather data from the European Centre for Medium-Range Weather Forecasts (ECMWF) collected over the past decade [19]. This approach is also being applied in the Orcelle project [20] and is integral to the current study.

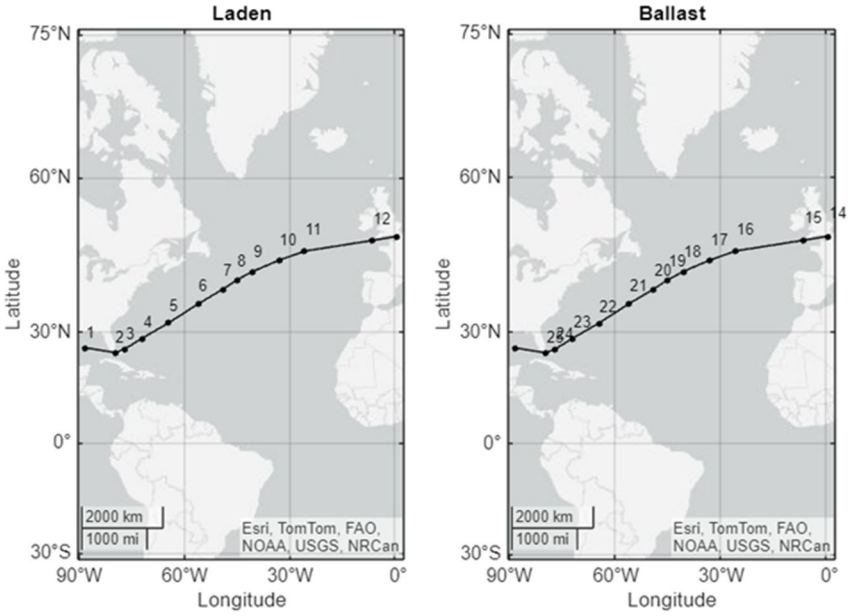

Figure 2. Selected route from Corpus Christi (USA) to Rotterdam (the Netherlands).

2.2. Wing Sail Characteristics

The primary objective of this methodology is to develop tools for evaluating the impact of WAPSs on ship design within a design concept optimization framework. The wing sail system examined in this study is based on a simplified, generic arrangement of symmetrical NACA airfoils [21]. This configuration is significantly different from the Orcelle Oceanbird concept [22], which features an optimized main wing with a controllable flap. The herein-adopted approach enables the development of WAPS simulation tools independently of the Oceanbird concept's design and efficiency. The Oceanbird configuration, expected to provide higher lift and thrust efficiency, is planned to be incorporated into the simulation tools in future studies.

In this context, the WAPS analyzed here comprises eight rigid wing sails, each approximately 80 m in height with an average chord length of 23 m. The wing profile is assumed to be an NACA0015 airfoil with a modified trailing edge. Each sail has a surface area of 1844 m^2, a mean chord length of 23 m, and an aspect ratio of 3.47 [23]. The MATLAB simulation code developed for this study is designed to accommodate variations in the number, arrangement, size, and profile of wing sails. Additionally, it can support alternative WAPS configurations, such as other types of wing sails or rotors, provided aerodynamic data are available for estimating the associated lift and drag forces.

In this case study, certain assumptions about the placement and interaction of the wing sails are made to simplify the problem, reduce computational time, and limit the number of variables in the optimization process. The positioning of the sails (both longitudinally and laterally) plays a critical role in maximizing their effectiveness. However, within the 1-DOF model, the exact placement of the sails is not analyzed. Instead, it is assumed that an optimized sail arrangement exists, which maximizes wind-generated thrust, minimizes the impact of drift angle and rudder resistance needed to maintain course, and meets all necessary requirements (e.g., bridge visibility, structural integrity, etc.) [24].

When the force generated by the sails is sufficient to propel the vessel at the desired speed (i.e., 100% wind-generated thrust), several options for propeller operation are available, such as windmilling, feathering, or energy harvesting [25]. However, for this optimization problem, energy harvesting from the rotating propeller is not considered, and the additional resistance caused by a windmilling or feathered propeller is also excluded from the analysis.

2.3. Estimation of Forces

The developed model focuses on simulating longitudinal (surge) forces. To achieve this, the voyage is segmented into legs, each with constant speed and environmental conditions. For each leg, Equation (1) is applied to calculate the thrust generated by the propeller.

$$X_{CW} + X_{AW} + X_W + X_S + T = 0 \quad (1)$$

X_{CW} is the calm water resistance (N), which is calculated using the Holtrop and Mennen method [26,27], properly calibrated to predict the calm water resistance of the reference vessel.

X_{AW} is the added resistance due to waves (N), which is calculated using the semi-empirical SNNM method [28].

X_W is the wind resistance (N) of the ship's superstructure, which is estimated according to ISO 15016 [29].

X_S is the generated sail force (N) for the assumed wing sails, which is calculated from tabulated aerodynamic forces provided by RISE Research Institutes of Sweden (personal communication).

T is the propeller thrust (N).

2.4. Vessel Performance Comparison with and Without Sails

The developed tool can simulate the entire voyage, performing detailed calculations for each leg and enabling a direct comparison between the same vessel design with and without sails. Below, some representative figures are provided, showcasing the results from the various modules (hull, engine, propeller, and sail). The figures specifically refer to the 20th leg of the selected voyage for the reference vessel (Figure 3).

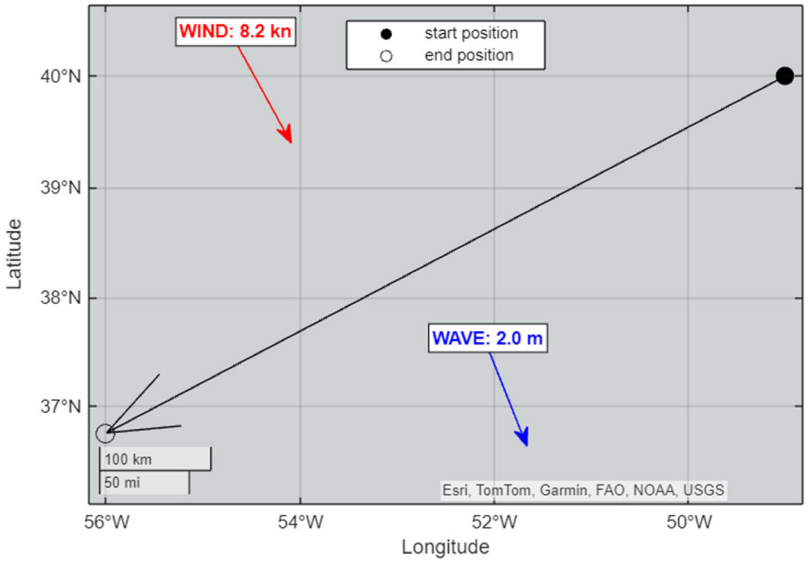

Figure 3. Weather characteristics of leg 20 of the selected route.

2.4.1. Forces

For each leg, all the forces are calculated (Figure 4), and the percentages of propulsion and resistance forces are depicted in Figure 5.

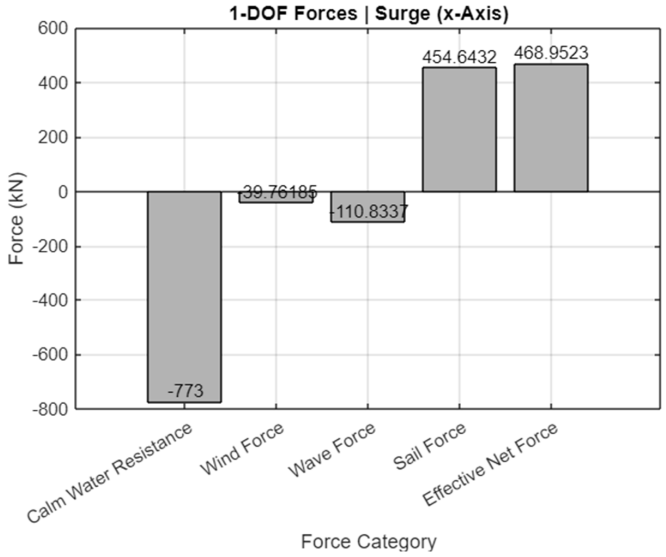

Figure 4. Estimated forces for leg 20 of the selected route.

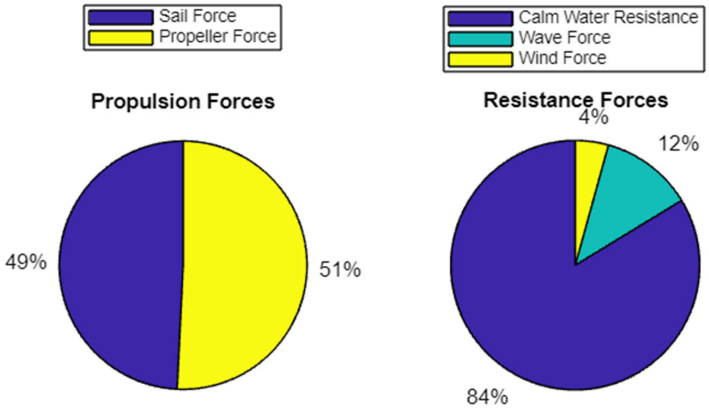

Figure 5. Force percentages for leg 20 of the selected route.

2.4.2. Hull

The calm water resistance of the vessel is plotted in Figure 6, along with the operational points. Speed is fixed to 12 knots.

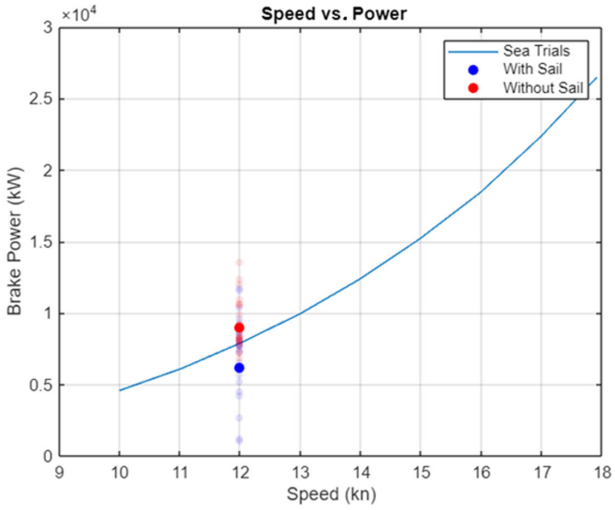

Figure 6. Speed vs. resistance (solid points refer to leg 20 of the selected route; transparent points refer to the data for the rest of the legs).

2.4.3. Main Engine

The engine layout diagram and the calculated operational points for all voyage legs are presented in Figure 7, while the Specific Fuel Oil Consumption (SFOC) is shown in Figure 8. It is important to note that the engine is assumed to remain in operation at all times (i.e., zero brake power is not permitted). In practice, very low engine loads [30] need to be addressed through an operational strategy, such as increasing vessel speed or adjusting sail trim, to avoid operating at such low loads with correspondingly high SFOC. However, in the optimization conducted for this study, this factor was not considered, as most operational points in the examined case study do not require extremely low engine loads. As a result, the influence of such operational strategies on the optimization results is minimal.

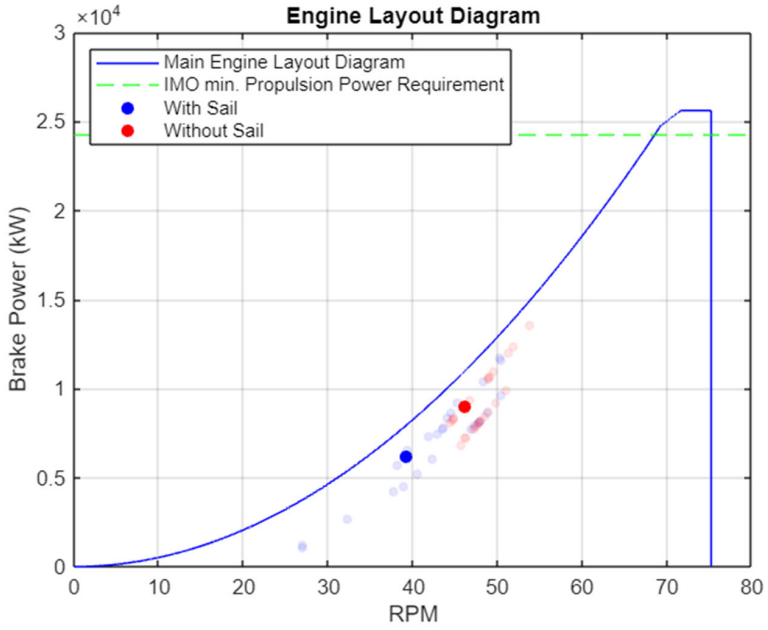

Figure 7. Engine layout diagram (solid points refer to leg 20; transparent points refer to the rest of the legs).

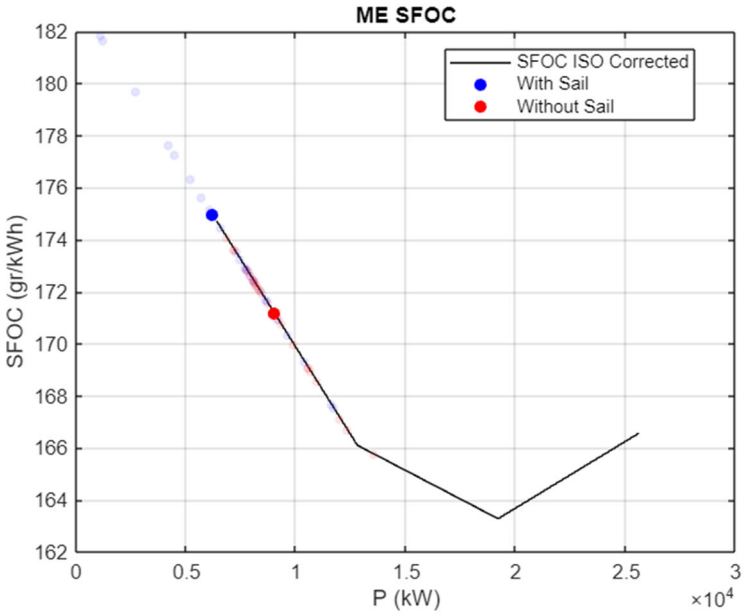

Figure 8. Power vs. Specific Fuel Oil Consumption (SFOC) (solid points refer to leg 20; transparent points refer to the rest of the legs).

2.4.4. Propeller

The study vessel is herein assumed to be equipped with a Fixed Pitch Propeller (FPP), even though in practice, WAPS ships will be generally equipped with Controllable Pitch Propellers (CPPs), better accounting for the varying effect of WAPSs on propeller and engine loading. In this study, the fitted FPP is modeled using the polynomials of the Wageningen B-series [31,32]. Propeller efficiency is calculated for various operating points (Figure 9), and a verification is performed to ensure that excessive cavitation does not occur (Figure 10).

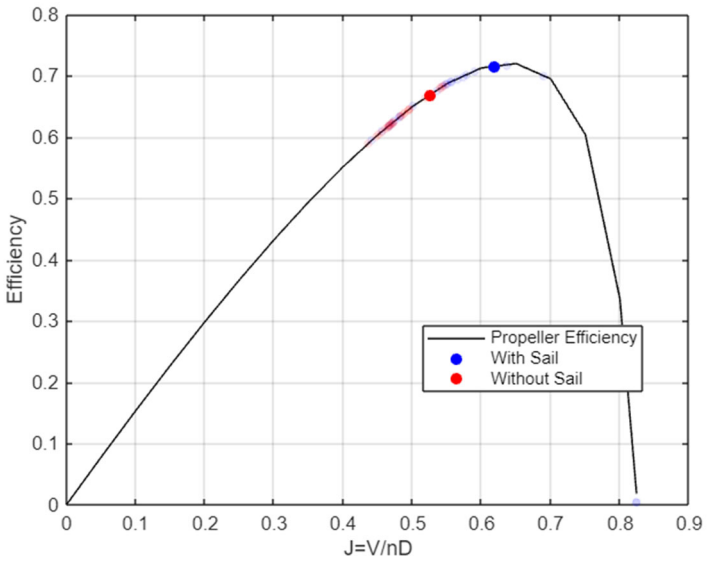

Figure 9. Propeller efficiency (solid points refer to leg 20; transparent points refer to the rest of the legs).

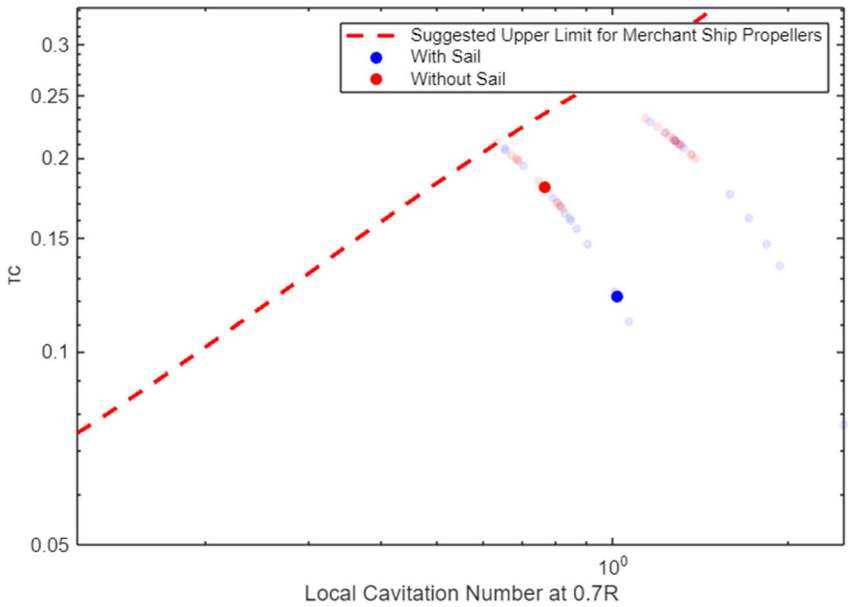

Figure 10. Checking for cavitation [33] (solid points refer to leg 20; transparent points refer to the rest of the legs).

2.4.5. Wing Sail

For the wing sail, the forces are determined based on the apparent wind speed, apparent wind angle, and the lift/drag characteristics of the corresponding wing profile (Figure 11).

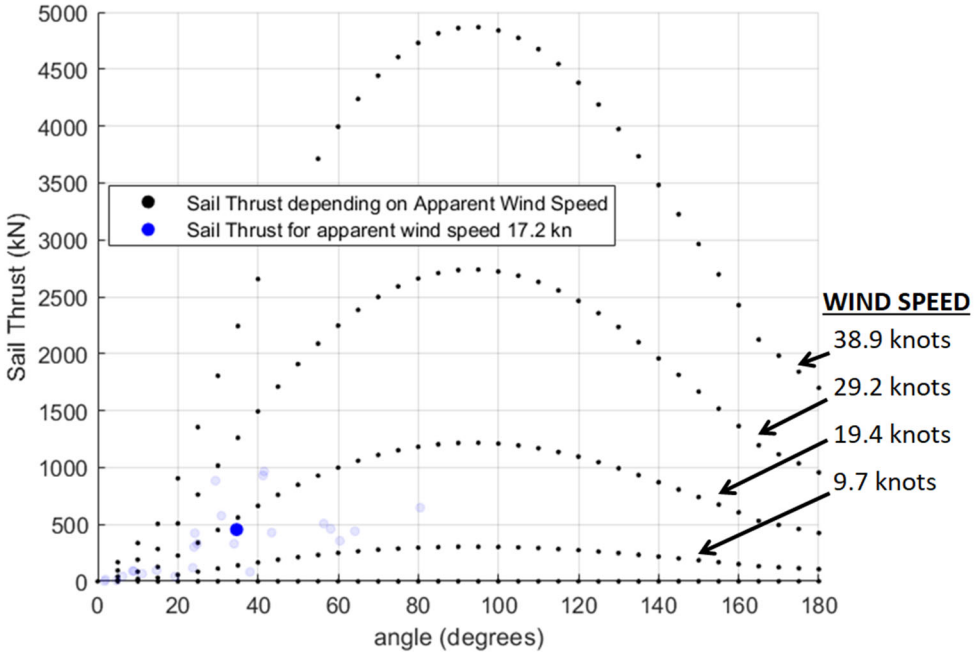

Figure 11. Wing sail thrust (8 wing sails) depending on wind angle and wind speed.

3. Design Optimization Methodology

A tailored optimization problem has been formulated specifically for the design of ships equipped with WAPSs, along with the development of an appropriate methodology to address the wind-assisted propulsion challenge. The optimization process aims to determine the optimal combination of hull, engine, and propeller that minimizes the objective functions while accounting for the impact of the examined WAPS. The optimization module, coded in MATLAB, supports both single- and multi-objective optimization studies, with the overall process outlined in Figures 12 and 13. The current study focuses on a multi-objective optimization problem, and some key details of the optimization process are briefly highlighted below.

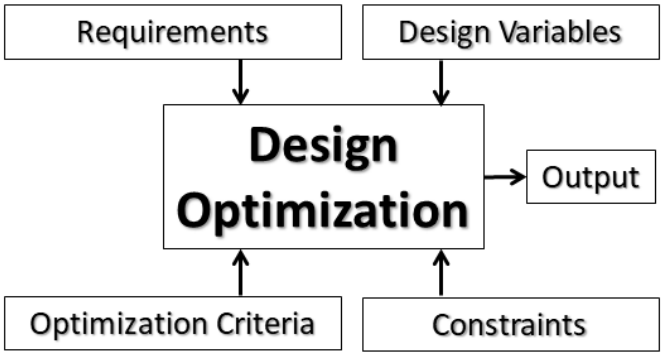

Figure 12. Generic design optimization process [34,35].

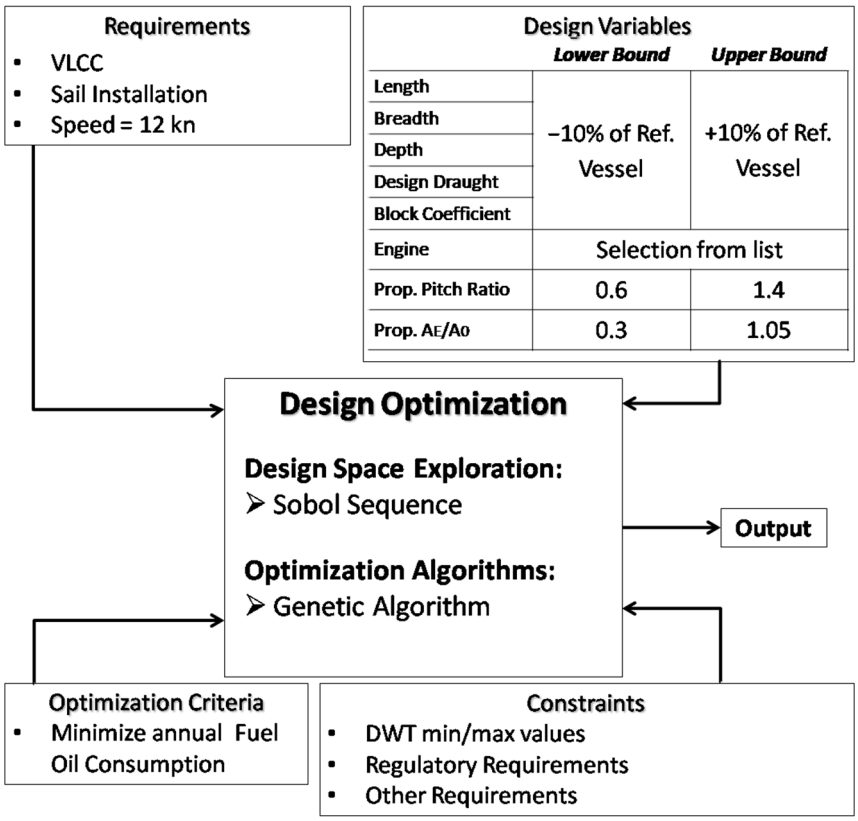

Figure 13. WAPS optimization process for VLCC case study.

3.1. Design Space Exploration

To ensure a thorough exploration of the design space, a large number of initial designs are generated using the SOBOL sequence [36]. This probabilistic sampling method provides more uniform coverage of the design space compared to a pseudorandom number generator. It enhances population diversity and contributes to improved optimization outcomes [37]. In the case study presented, 2000 designs are generated, and the top 50 feasible designs are selected to form the initial population for the genetic algorithm (Figure 14).

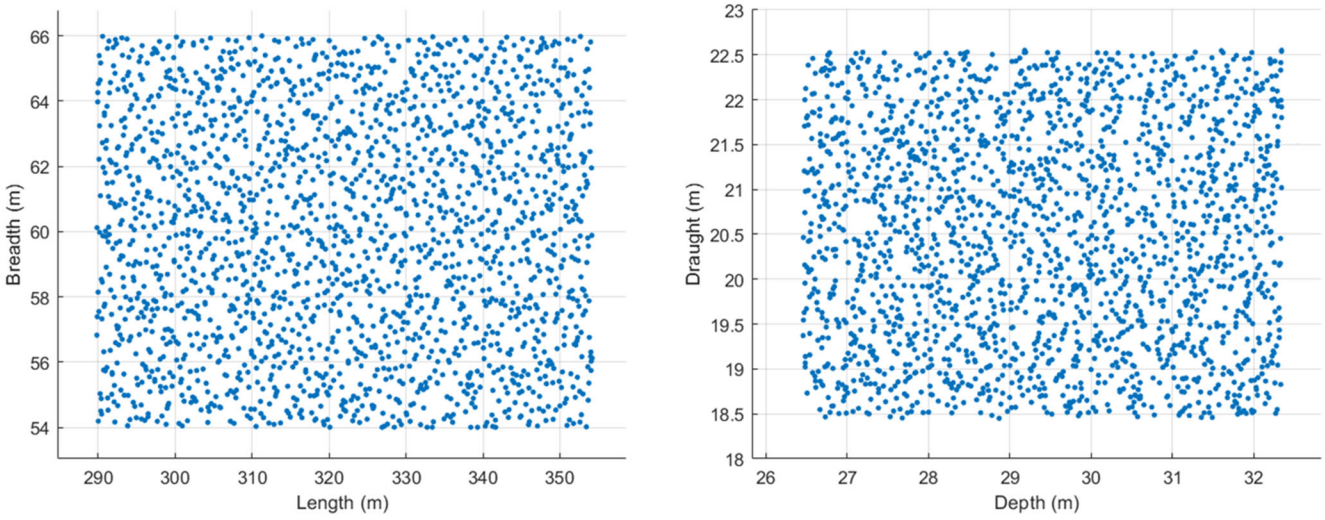

Figure 14. Initial 2000 designs using SOBOL sequence.

3.2. Heuristic Optimization Algorithm

The global optimization algorithm that is utilized is the genetic algorithm. We optimize for 200 generations with each generation containing 50 individuals.

4. Implementation

The developed WAPS simulation tool is integrated into the previously defined design optimization methodology to address the wind-assisted design optimization problem in a comprehensive manner. Key aspects of the methodology's implementation are briefly outlined below.

4.1. Design Variables

In the application study presented here, we consider 8 ship design variables: length (L), breadth (B), depth (D), draught (T), block coefficient (CB), engine BHP/type (chosen from a list), propeller pitch ratio (P/D), and propeller expanded area ratio (AE/A0). To enhance the efficiency of the genetic algorithm used for optimization, all design variables are treated as integers (discrete optimization). For L, B, D, and T, we retain two decimal places, so L_integer = L·100, B_integer = B·100, etc. For CB, P/D, and AE/A0, we maintain three decimal places (CB_integer = CB·1000, etc.). The engine selection parameter is also an integer that corresponds to the engine chosen from the provided list. This approach significantly accelerates the optimization process and facilitates a more comprehensive exploration of the design space.

4.2. Multi-Objective Functions

The objective functions used in this case study are the minimization of the annual fuel oil consumption of the main engine (which indirectly reduces associated GHG emissions) and the minimization of the Required Freight Rate (RFR). The objective functions are estimated based on the specific routing and the associated weather conditions. The annual fuel consumption is then calculated by considering the reference vessel's year-round voyage plan, including the yearly percentage of laden and ballast sailing time, as well as the number of round trips the vessel can complete annually.

4.3. Constraints

The design optimization problem incorporates 15 constraints to ensure that the resulting designs are feasible. Specifically, these constraints include limits for the Deadweight Tonnage (DWT), form coefficients, and main dimension ratios to ensure that the generated designs are practical and closely aligned with data from existing vessels [38]. The constraints also ensure that the propeller operates within engine limits while minimizing cavitation [39], and that the designs comply with regulations regarding freeboard [40] and minimum propulsion power [41]. A minimum metacentric height (GM) of 3 m is required as an initial control check for the vessel's intact stability.

The constraints applied to the VLCC tanker considered in this study are summarized below:

1. Min. DWT $\geq$ 263,060 tons ($-$5% from reference vessel);
2. Max. DWT $\leq$ 290,750 tons (+5% from reference vessel);
3. Engine limit constraint;
4. Less than approximately 5% cavitation at the propeller;
5. $0.79 \leq CB \leq 0.88$;
6. $0.992 \leq CM \leq 0.996$;
7. $0.88 \leq CWL \leq 0.94$;
8. $0.835 \leq CP \leq 0.855$;

9. $5.1 \leq L/B \leq 6.8$;
10. $2.4 \leq B/T \leq 3.2$;
11. $10.5 \leq L/D \leq 14$;
12. IMO minimum power requirement;
13. Freeboard constraint;
14. GM $\geq$ 3 m;
15. $0.2 \cdot T \leq$ propeller diameter $\leq 0.55 \cdot T$.

5. Case Study

5.1. Reference Vessel

The reference vessel is an existing VLCC tanker. The main particulars of the reference vessel are presented in Table 1.

Table 1. Main particulars of reference vessel.

Length B.P.	322.00 m
Breadth Mld.	60.00 m
Depth Mld.	29.40 m
Design Draught	20.50 m
CB	0.796
RFR (USD/ton cargo)	8.27
Annual Fuel Cons. (tons)	13,253

5.2. Selected Route and Weather Characteristics

The selected route for the case study is a common route from Corpus Christi (USA) to Rotterdam (Figure 2). The weather characteristics per leg were provided by the ORCELLE partner StormGEO, Bergen, Norway [42] and contain ERA5 data from 2022. ERA5 [43] is the fifth-generation atmospheric reanalysis of the global climate, produced by the Copernicus Climate Change Service (C3S) at ECMWF. Seasonal changes in weather are taken into consideration by simulating multiple scenarios within 2022. More specifically, instead of simulating the voyage for the average weather conditions that prevail in each waypoint, 24 actual weather scenarios are simulated for the same route by assuming different start dates of the voyage. This results in an average year-round fuel consumption estimation which provides a more realistic picture of the expected fuel consumption based on actual weather conditions and not on average values.

It is important to note that the integration of WAPSs should be considered alongside weather routing optimization. As such, the conventional route examined (which is not optimized for prevailing winds) considerably underestimates the potential savings [44].

6. Results

The optimization algorithm results are shown in Table 2, while Figure 15 provides a comparison of the initial population (both feasible and infeasible), the reference vessel (with and without sails), and the optimized vessels.

Table 2. Optimum designs (Pareto front).

L (m)	B (m)	D (m)	T (m)	CB	CM	Engine MCR (kW)	P/D	AE/A0	Annual Fuel Cons. (Tons)	RFR (USD/Ton Cargo)
327.22	56.63	28.96	21.57	0.789	0.998	29,286	0.766	0.612	10,466.4	7.5
327.86	56.97	26.99	21.99	0.803	0.998	29,286	0.705	0.592	11,014.5	7.3
327.79	56.92	27.01	21.99	0.801	0.998	29,286	0.746	0.592	10,939.2	7.3

Table 2. *Cont.*

L (m)	B (m)	D (m)	T (m)	CB	CM	Engine MCR (kW)	P/D	AE/A0	Annual Fuel Cons. (Tons)	RFR (USD/Ton Cargo)
327.37	56.66	28.79	21.71	0.789	0.998	29,286	0.757	0.596	10,508.1	7.5
327.39	56.64	28.79	21.85	0.789	0.998	29,286	0.757	0.596	10,539.0	7.4
327.59	56.85	26.98	21.98	0.798	0.998	29,286	0.752	0.59	10,855.8	7.3
327.64	56.64	28.56	21.93	0.79	0.998	29,286	0.762	0.597	10,592.5	7.4
327.61	56.66	27.12	21.93	0.79	0.998	29,286	0.757	0.593	10,644.1	7.4
327.61	56.76	27.07	21.98	0.795	0.998	29,286	0.739	0.593	10,780.2	7.3
327.65	56.75	27.13	21.98	0.793	0.998	29,286	0.75	0.595	10,737.5	7.3
327.43	56.72	27.28	21.91	0.793	0.998	29,286	0.759	0.593	10,698.8	7.4
327.43	56.66	28.21	21.86	0.789	0.998	29,286	0.758	0.596	10,568.4	7.4
327.59	56.88	27.13	21.99	0.8	0.998	29,286	0.726	0.593	10,910.7	7.3
327.32	56.63	28.86	21.66	0.789	0.998	29,286	0.761	0.601	10,486.9	7.5
327.63	56.61	28.73	21.6	0.789	0.998	29,286	0.777	0.599	10,480.1	7.5
327.64	56.65	28.2	21.94	0.791	0.998	29,286	0.756	0.596	10,626.7	7.4
327.71	56.86	26.99	21.98	0.799	0.998	29,286	0.744	0.591	10,881.7	7.3
327.78	56.76	27.04	21.99	0.796	0.998	29,286	0.746	0.592	10,801.8	7.3

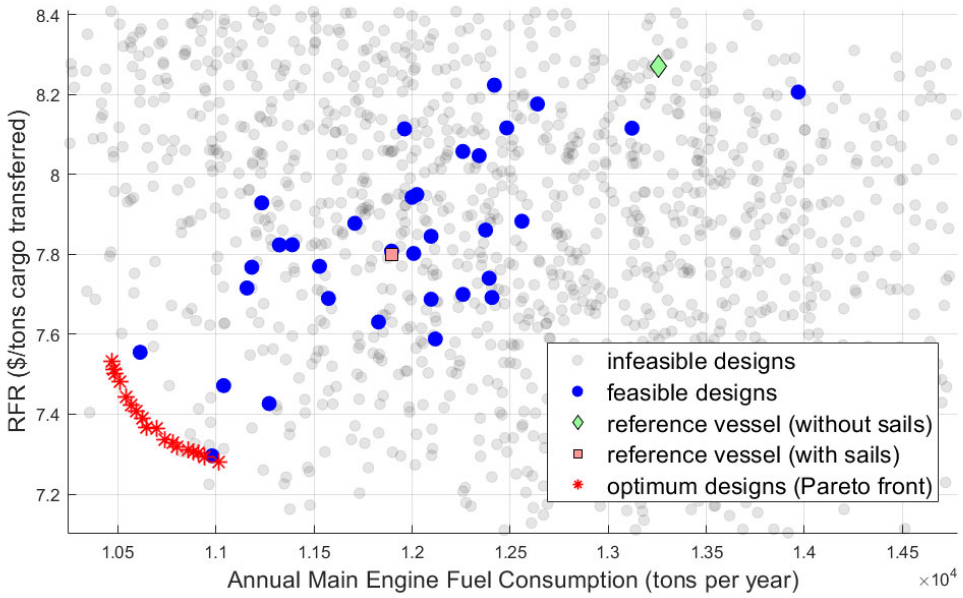

Figure 15. Comparison of design alternatives and optimization results.

Figure 15 illustrates that during the design exploration phase, a considerable number of infeasible designs (represented by gray points) were generated, highlighting the influence of the defined initial design conditions and constraints. The outcome underscores the importance of having a sufficiently large and evenly distributed initial design population to ensure that the optimization algorithm converges to the global optimum. The optimized designs exhibit reduced breadth and greater draught. These design characteristics have a positive effect on the sail thrust-to-resistance ratio [14]. In addition, the optimized designs show improvements in calm water resistance and hull efficiency coefficient, as well as in the added wave resistance, thus contributing to the overall performance enhancement, even without the incorporation of sails. A detailed analysis of the optimized designs along the Pareto front reveals that larger vessels exhibit improved RFR, while smaller vessels show reductions in fuel consumption, as anticipated. It is worth noting that the ±5% constraint on deadweight DWT relative to the reference vessel allows the displacement to vary accordingly, provided the DWT remains within the prescribed range. It is also interesting to note that if the present wing sail system were installed at the reference vessel

(retrofitting), the estimated annual main engine consumption would be 11895 tons (instead of 13,253 tons—appr. 10% improvement). For the RFR, the improvement is 5%. Compared to the original vessel (green point in Figure 15), multi-optimized designs are more than 20% better in terms of fuel consumption (and associated emissions), and likewise in terms of RFR. It should be finally noted that the effect of the WAPS on the ship's main dimensions can be expected to be more drastic for other ship types and sizes, and thus in general for volume carriers (like car carriers) compared to deadweight carriers (tankers and bulkers); in other words, considering the same wind potential for all ships operating on the same route, its effect on a ship's propulsion (and motions) will be directly dependent on the ship's size (and displacement), and thus on the magnitude of the generated wind thrust compared to the ship's total resistance. A schematic diagram of the wind-assisted VLCC designed in NAPA [45] is depicted in Figure 16.

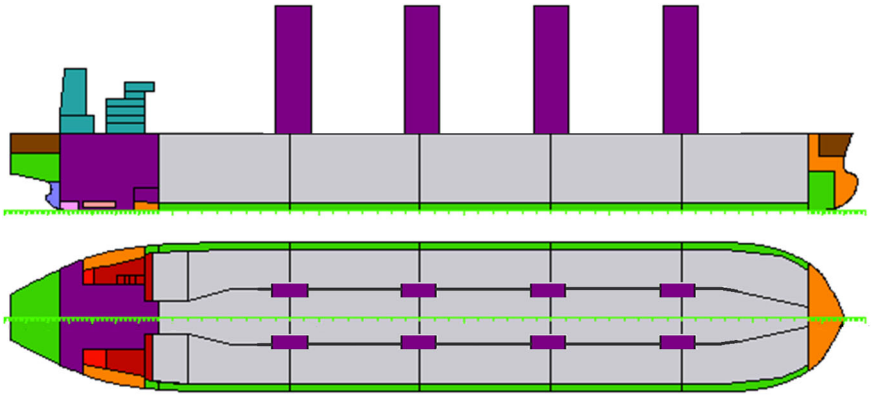

Figure 16. Schematic diagram of wind-assisted VLCC.

7. Summary and Conclusions

This paper introduces a newly developed simulation tool designed to evaluate the performance of ships equipped with WAPSs and to analyze the impact of wing sails on ship concept design within a multi-parametric optimization framework. The tool was applied to a case study involving a VLCC tanker, yielding several key conclusions:

1. The optimized VLCC tankers with WAPSs exhibit characteristics significantly different from conventional VLCC designs without WAPSs. Optimized designs tend to be slightly more slender and deeper. The observed design characteristics have a positive effect on sail thrust, as well as on calm water resistance and added wave resistance. These differences are likely to be even more pronounced for smaller vessels or other ship types, particularly when comparing volume carriers versus deadweight carriers.
2. The estimated fuel savings (and GHG emissions reduction) and RFR improvement for the VLCC tanker are notable. Compared to the original vessel, multi-optimized designs showed an improvement of approximately 20% in terms of fuel consumption (and associated emissions), and likewise in terms of RFR. While these results may seem optimistic due to the simplified 1-DOF hydrodynamic modeling used, greater savings may be realized by optimizing the route for wind potential and utilizing advanced wing sail technologies, such as the Oceanbird concept, rather than the generic NACA wing profiles used in this study
3. Ship design and operational parameters, including main dimensions, engine and propeller characteristics, route, speed, wing sail size/number/arrangement, logistics, and WAPS alternatives, all play a critical role when a ship is fitted with a WAPS. These factors must be integrated into a holistic ship design optimization process.

It is evident that considering only (and separately) the performance of specific WAPSs, specific routes, and specific ship and WAPS arrangements will not fully uncover the potential of WAPSs. Thus, multi-parametric ship design optimization frameworks, including parameters specifying the WAPSs, as well as their effect in the main particulars and basic design characteristics, with a multitude of objectives and constraints, play a crucial role in the concept design of a vessel in order to fully exploit WAPSs. The above holistic approach to wind-assisted ship design is essential to fully tap the potential of WAPSs and promote their widespread adoption in the maritime industry.

Author Contributions: T.P.: conceptualization; data curation, methodology; writing—original draft. A.P.: conceptualization; supervision; writing—review and editing. All authors have read and agreed to the published version of the manuscript.

Funding: This research was funded by European Union/HORIZON CL-5, contract number 101096673.

Institutional Review Board Statement: Not applicable.

Informed Consent Statement: Not applicable.

Data Availability Statement: Data is contained within the article.

Acknowledgments: The support of this research by the European Commission research project ORCELLE WIND under the European Union's Horizon research and innovation program under grant agreement n° 101096673 is acknowledged. Also, the early support by the RTD project HOLISHIP [46] under the European Union's Horizon research and innovation program under grant agreement n° 689074 is acknowledged. The European Commission and the authors shall not in any way be liable or responsible for the use of any knowledge, information or data presented, or of the consequences thereof. The authors also acknowledge the support of the ORCELLE WIND project partners SSPA/RISE and StormGeo for the provision of aerodynamic data on wing sail performance and weather data pertaining to the presented case study, respectively. The provision of comparative ship data for the conducted case study by THENAMARIS is also acknowledged.

Conflicts of Interest: The authors declare no conflict of interest.

References

1. European Maritime Safety Agency. *Potential of Wind-Assisted Propulsion for Shipping*; EMSA: Lisbon, Portugal, 2023.
2. International Maritime Organization. *Resolution MEPC.351(78)—2022 Guidelines on Survey and Certification of the Attained Energy Efficiency Existing Ship Index (EEXI)*; International Maritime Organization: London, UK, 2022.
3. International Maritime Organization. *Resolution MEPC.352(78)—2022 Guidelines on Operational Carbon Intensity Indicators and the Calculation Methods (CII Guidelines, G1)*; International Maritime Organization: London, UK, 2022.
4. International Maritime Organization. *ResolutionMEPC.364(79), 2022 Guidelines on the Method of Calculation of the Attained Energy Efficiency Design Index (EEDI) for New Ships*; International Maritime Organization: London, UK, 2022.
5. International Windship Association (IWSA). *Wind Propulsion: Zero-Emissions Energy Solution for Shipping*; IWSA: London, UK, 2024.
6. Hansen, K.E.; Bloch, M.R.; Jens, O.V. *Modern Windships*; Technical Report; Pelmatic Knud E. Hansen A/S: Copenhagen, Denmark, 2000.
7. Bentin, M.; Kotzur, S.; Schlaak, M.; Zastrau, D.; Freye, D. Perspectives for a Wind Assisted Ship Propulsion. *Int. J. Marit. Eng.* **2018**, 160. [CrossRef]
8. Talluri, L.; Nalianda, D.K.; Giuliani, E. Techno economic and environmental assessment of Flettner rotors for marine propulsion. *Ocean. Eng.* **2018**, *154*, 1–15. [CrossRef]
9. Viola, I.M.; Sacher, M.; Xu, J.; Wang, F. A numerical method for the design of ships with wind-assisted propulsion. *Ocean. Eng.* **2015**, *105*, 32–42. [CrossRef]
10. Ma, R.; Wang, Z.; Wang, K.; Zhao, H.; Jiang, B.; Liu, Y.; Xing, H.; Huang, L. Evaluation Method for Energy Saving of Sail-Assisted Ship Based on Wind Resource Analysis of Typical Route. *J. Mar. Sci. Eng.* **2023**, *11*, 789. [CrossRef]
11. Tillig, F.; Ringsberg, J. A 4 DOF simulation model developed for fuel consumption prediction of ships at sea. *Ships and Offshore Structures* **2019**, *14* (Suppl. S1), S112–S120. [CrossRef]

12. Lu, R.; Ringsberg, J.W. Ship energy performance study of three wind-assisted ship propulsion technologies including a parametric study of the Flettner rotortechnology. *Ships Offshore Struct.* **2019**, *15*, 249–258. [CrossRef]
13. Guzelbulut, C.; Badalotti, T.; Suzuki, K. Optimization techniques for the design of crescent-shaped hard sails for wind-assisted ship propulsion. *Ocean. Eng.* **2024**, *312*, 119142. [CrossRef]
14. Hao, Z.; Ouyang, X.; Chen, J.; Wu, W.; Chen, L.; Feng, Y. Multiobjective optimization of low-speed sail-assisted VLCC performance. *Ocean. Eng.* **2024**, *312 Pt 1*, 119327. [CrossRef]
15. Plessas, T.; Papanikolaou, A. Optimization of Ship Design for the Effect of Wind Propulsion. In Proceedings of the 15th International Marine Design Conference (IMDC-2024), Amsterdam, The Netherlands, 2–6 June 2024.
16. MATLAB. Mathworks. 2024. Available online: www.mathworks.com (accessed on 1 July 2024).
17. Papanikolaou, A.; Fournarakis, N.; Chroni, D.; Liu, S.; Plessas, T.; Sprenger, F. Simulation of the Maneuvering Behavior of Ships in Adverse Weather Conditions. In Proceedings of the 31st Symposium on Naval Hydrodynamics, Monterey, CA, USA, 11–16 September 2016.
18. NAPA. 2024. Available online: www.napa.fi (accessed on 1 July 2024).
19. Werner, S.; Kuttenkeuler, J.; Hörteborn, A. Route Evaluation Methods for Long-Distance Sailing Vessel Performance Predictions. In Proceedings of the 7th High Performance Yacht Design Conference, Auckland, New Zealand, 11–12 March 2021.
20. ORCELLE (2023–2027) European Union/HORIZON CL-5, contract number 101096673. Available online: https://cordis.europa.eu/project/id/101096673 (accessed on 1 July 2024).
21. Abbott, I.H.; VonDoenhoff, A.E. *Theory of Wing Sections*; Dover Publications: New York, NY, USA, 1959.
22. Oceanbird. 2024. Available online: www.theoceanbird.com (accessed on 1 July 2024).
23. Malmek, K.; Dhome, U.; Larsson, L.; Werner, S.; Ringsberg, J.W.; Finnsgard, C. Comparison of Two Rapid Numerical Methods for Predicting the Performance of Multiple Rigid Wing-Sails. In Proceedings of the 5th INNOV'SAIL Conference, Gothenburg, Sweden, 15–17 June 2020.
24. Bordogna, G.; Keuning, J.A.; Huijsmans, R.H.M.; Belloli, M. Wind-tunnel experiments on the aerodynamic interaction between two rigid sails used for wind-assisted propulsion. *Int. Shipbuild. Prog.* **2018**, *65*, 93–125. [CrossRef]
25. Gypa, I.; Jansson, M.; Gustafsson, R.; Werner, S.; Bensow, R. Controllable-pitch propeller design process for a wind-powered car-carrier optimising for total energy consumption. *Ocean. Eng.* **2023**, *269*, 113426. [CrossRef]
26. Holtrop, J.; Mennen, G.G.J. An Approximate Power Prediction Method. *Int. Shipbuild. Prog.* **1982**, *29*, 166–170. [CrossRef]
27. Holtrop, J. A statistical Re-Analysis of Resistance and Propulsion Data. *Int. Shipbuild. Prog.* **1984**, *31*, 363.
28. Liu, S.; Papanikolaou, A. Regression analysis of experimental data for added resistance in waves of arbitrary heading and development of a semi-empirical formula. *Ocean. Eng.* **2020**, *206*, 107357. [CrossRef]
29. *ISO15016*; Ships and Marine Technology—Guidelines for the Assessment of Speed and Power Performance by Analysis of Speed Trial Data. International Organization for Standardization: Geneva, Switzerland, 2015.
30. Reche-Vilanova, M.; Bingham, H.B.; Psaraftis, H.N.; Fluck, M.; Morris, D. Preliminary Study on the Propeller and Engine Performance Variation with Wind Propulsion Technologies. In Proceedings of the WindPropulsion Conference 2023, London, UK, 16–17 February 2023.
31. Lammeren, W.P.A.; van Manen, J.D.; Oosterveld, M.W.C. The Wageningen B-screw series. *Trans. SNAME* **1969**, *269*.
32. Oosterveld, M.W.C.; Van Oossanen, P. Further computer-analyzed data of the Wageningen B-screw series. *Int. Shipbuild. Prog.* **1975**, *22*, 251–262. [CrossRef]
33. Carlton, J.S. *Marine Propellers and Propulsion, Butterworth-Heinemann*; Elsevier: Amsterdam, The Netherlands, 2007.
34. Papanikolaou, A. Holistic Ship Design Optimization. *J. Comput.-Aided Des.* **2010**, *42*, 1028–1044. [CrossRef]
35. Papanikolaou, A. (Ed.) *A Holistic Approach to Ship Design | Volume 1: Optimisation of Ship Design and Operation for Life Cycle*; Springer: Berlin/Heidelberg, Germany, 2019.
36. Bratley, P.; Fox, B.L. Algorithm 659 Implementing Sobol's Quasi random Sequence Generator. *ACM Trans. Math. Softw.* **1988**, *14*, 88–100. [CrossRef]
37. Agushaka, J.O.; Ezugwu, A.E. Initialisation Approaches for Population-Based Metaheuristic Algorithms: A Comprehensive Review. *Appl. Sci.* **2022**, *12*, 896. [CrossRef]
38. Papanikolaou, A. *Ship Design Methodologies of Preliminary Design*; Springer: Berlin/Heidelberg, Germany, 2014.
39. Burrill, L.C.; Emerson, A. Propeller cavitation: Further tests on 16 in. propeller models in the King's College Cavitation Tunnel. *Trans. NECIES* **1963**, *10*, 119–131. [CrossRef]
40. International Maritime Organization. *Convention on Load Lines*; International Maritime Organization: London, UK, 1966.
41. International Maritime Organization. *Guidelines for Determining Minimum Propulsion Power to Maintain the Manoeuvrability of Ships in Adverse Conditions*; MEPC.1/Circ.850/Rev.3, 2021; International Maritime Organization: London, UK, 2021.
42. StormGeo, Bergen, Norway. 2024. Available online: www.stormgeo.com (accessed on 1 July 2024).
43. Hersbach, H.; Bell, B.; Berrisford, P.; Hirahara, S.; Horányi, A.; Muñoz-Sabater, J.; Nicolas, J.; Peubey, C.; Radu, R.; Schepers, D.; et al. The ERA5 global reanalysis. *Q. J. R. Meteorol. Soc.* **2020**, *146*, 1999–2049. [CrossRef]

44. Werner, S.; Papanikolaou, A.; Razola, M.; Fagergren, C.; Dessen, L.; Kuttenkeuler, J.; Santen, V.; Steinbach, C. The Orcelle project—Towards Wind-Powered Ships for Deep Sea Cargo Transport. In Proceedings of the SNAME Maritime Convention 2023, San Diego, CA, USA, 27–29 September 2023.
45. Kanellopoulou, A. Parametric Ship Design and Optimization. Ph.D. Thesis, National Technical University of Athens, Athens, Greece, July 2023.
46. HOLISHIP (2016-2020), HORIZON 2020—EU funded project, Grant Agreement n° 689074. Available online: http://www.holiship.eu/ (accessed on 1 July 2024).